PAPER Nr. : 31

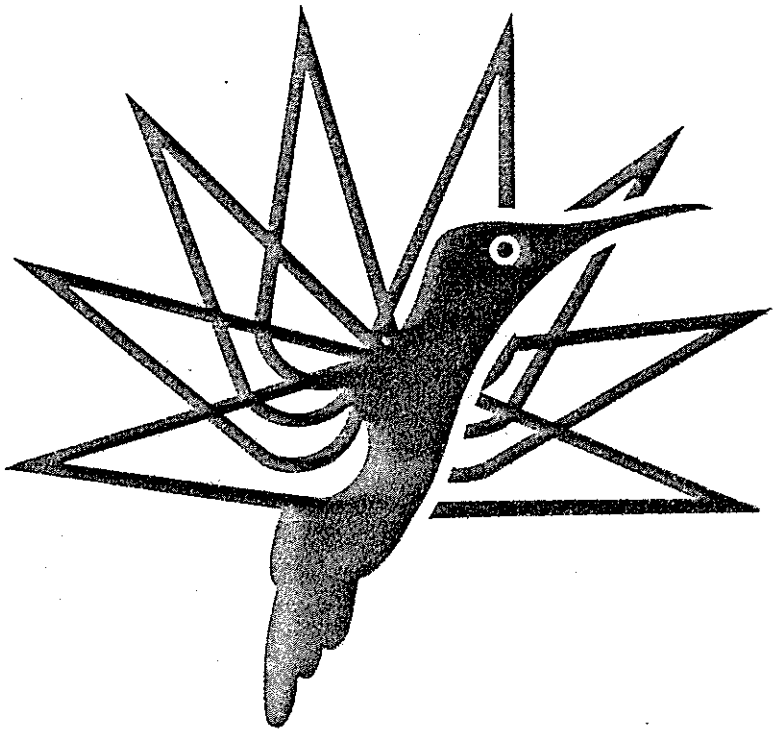

A METHOD OF HELICOPTER LOW AIRSPEED ESTIMATION BASED ON MEASUREMENT OF CONTROL PARAMETERS

by

A.J. Faulkner, S. Attlfellner

Messerschmitt-Bölkow-Blohm GmbH
Munich, Germany

FIFTH EUROPEAN ROTORCRAFT AND POWERED LIFT AIRCRAFT FORUM
SEPTEMBER 4 – 7TH 1979 - AMSTERDAM, THE NETHERLANDS

A METHOD OF HELICOPTER LOW AIRSPEED ESTIMATION BASED ON MEASUREMENT OF CONTROL PARAMETERS

A.J. Faulkner, S. Attlfellner

Messerschmitt-Bölkow-Blohm GmbH
Munich, Germany

Abstract

Significant changes in handling qualities, during low speed flight and hover, contribute towards making this flight state one of the most arduous for the helicopter pilot. This situation could be improved if the pilot was presented with an indication of airspeed and side-slip angle. The conventional pitot-static instrument operates inadequately, if at all, in this region and cannot be relied upon to give a representative indication of airspeed. To overcome the problems of conventional instruments, a number of devices, usually based on the pitot-static principle, have been specially developed, in the past, with varying degrees of success.

This paper describes an alternative indirect method of airspeed estimation, particularly suitable for the modern hingeless rotor helicopter, based on measurement of control and other parameters, most of which are readily available in a flight control system. A much simplified mathematical model of the helicopter rotor is discussed and analytic equations for the longitudinal and lateral aerodynamic velocity components are derived. Simulation results are presented and a practical system suggested.

Notation

a		Blade lift-curve slope
a_β	[m]	Flapping hinge offset
c_T		$= T / \frac{1}{2}\rho \cdot \pi \cdot R^2 (\Omega \cdot R)^2$, thrust coefficient
c	[m]	Blade chord
c_L		Blade profile lift coefficient
c_β	[Nm/rad]	Flapping hinge stiffness
dL	[N]	Incremental blade lift
dm	[kg]	Mass of blade element
dr	[m]	Radial thickness of blade element
$d\psi$	[rad]	Blade azimuth increment
E_x, E_y		Glauert downwash factors
f_x, f_y, f_z		Functions used in the calculation of airspeed
I_β		Blade second moment of mass
n		Number of blades
n_β		$= \gamma/8$, blade mass number

p	[rad/s]	Roll rate
$\bar{p}$		$= p/\Omega$, non-dimensional roll rate
q	[rad/s]	Pitch rate
$\bar{q}$		$= q/\Omega$, non-dimensional pitch rate
R	[m]	Rotor radius
r	[m]	Blade radial coodinate
S_β		$(\bar{\omega}_\beta^2-1)/n_\beta$, blade stiffness number
T	[N]	Rotor thrust
U_P	[m/s]	Aerodynamic velocity perpendicular to blade element
U_T	[m/s]	Aerodynamic velocity tangential to blade element
V	[m/s]	Velocity
$\bar{V}$		$= V/\Omega \cdot R$, non-dimensional velocity
V	[m/s]	Total aerodynamic velocity relative to blade element
V_{Io}	[m/s]	Rotor induced velocity
V_x	[m/s]	Velocity, longitudinal axis
V_y	[m/s]	Velocity, lateral axis
V_z	[m/s]	Velocity, vertical axis
x		$= r/R$, non-dimensional blade coordinate
α	[rad]	Angle of attack
$\beta(\psi)$	[rad]	$\beta_o + \beta_{1s} \cdot \sin\psi + \beta_{1c} \cdot \cos\psi$, blade flapping angle
β_I	[rad]	Rotor in-built coning angle
γ		$= \rho \cdot c \cdot a \cdot R^4/I_\beta$ = Lock's number
Θ	[rad]	Helicopter pitch attitude
$\theta(\psi)$	[rad]	$= \theta_t + \theta_{1s} \cdot \sin\psi + \theta_{1c} \cdot \cos\psi$, blade pitch angle
θ_t	[rad]	In-built blade twist
ρ	[kg/m^3]	Air density
σ		$= n \cdot c \cdot R/\pi \cdot R^2$
ψ	[rad]	Blade azimuth position, zero at rear of disc
Ω	[rad/s]	Rotor angular velocity
ω_β	[rad/s]	Blade natural flapping frequency
$\bar{\omega}_\beta$		$= \omega_\beta/\Omega$, non-dimensional flapping frequency
$\cdot$		$= d/dt$
$'$		$= 1/\Omega \cdot d/dt$
$-$		Non-dimensional quantity

cation of any changes is observed from the attitude of the fuselage. Even at low forward speeds, pitch attitude changes are discernible owing to the fuselage aerodynamic drag. In fact, if no drag existed, pitch attitude changes would not be necessary. In roll, however, the mechanics are somewhat complicated by the tail rotor thrust, which attempts to balance the main rotor torque, and is therefore dependent on the power requirements of the main rotor. The trim of the helicopter therefore, in particular the pitch attitude, is basically governed by the fuselage aerodynamics or more precisely by the ratio of the aerodynamic drag to the weight of the aircraft.

The main rotor on the other hand, which produces the thrust and moment, is governed by completely different principles. The rotor is always operating, from an aerodynamic viewpoint, at high speed, even in the hover. The addition of the helicopter's forward speed, for example, must be considered as an extension of the existing flow round the blades. In hover, the helicopter pilot regulates the controls, collective and cyclic blade pitch, in order to produce the thrust and moment required for trim. At this stage, the collective control can be considered as varying the thrust magnitude and cyclic as varying the thrust direction relative to the rotor shaft. Owing to mass centre position and the lateral tail rotor thrust, however, the cyclic control is rarely in the central position in order to trim the hover.

To execute a forward manoeuvre, the pilot briefly moves the cyclic stick forward, deflecting the thrust direction and so resulting in a nose down pitching moment. The helicopter accelerates, thereby changing the aerodynamic flow conditions round the rotor and, in particular, increasing the resultant velocity on the advancing blade. The advancing blade experiences a greater lift force and flaps upward approximately 90° later; depending on the rotor "stiffness". The process can be viewed as a tilt of the rotor disc (tip-path plane), or in classical helicopter terminology as the "rotor flap-back". The result is that, as the helicopter accelerates, there is a tendency for the rotor to automatically supply a moment which acts to oppose the motion. This static speed stability characteristic is only overcome by the pilot adjusting cyclic pitch on the advancing blade (and an equal and opposite amount on the retreating blade) which he does by moving the cyclic stick forward as the airspeed increases.

The situation is further complicated, especially in the low speed region, by the rotor flow dissymmetry between the leading and trailing edges of the rotor disc. In hover, the induced flow can be reasonably assumed to be uniform across the whole rotor disc. With an increase in forward speed, this assumption becomes wildly inaccurate. In practice, the leading edge of the disc receives a reduced downwash (in some cases a slight up-wash) and the trailing edge an increased downwash. The distortion of the induced velocity field by the forward speed has long been recognised and a trapezoidal model of the phenomenon, originally suggested by Glauert, is often used in theoretical analyses, where the computing time involved in more advanced vortex models is prohibitive. Figure 2 compares a typical induced velocity distribution with the simple Glauert model. The result of distortion of the flow field is that the angle of attack of a blade in the forward edge of the rotor disc is increased, thus producing an increase in lift. Taking into account the phase lag between the application of the aerodynamic force and blade flapping motion, maximum disc tilt is observed in the retreating blade

1. Introduction

The development of the helicopter, following on from experience in the fixed wing field, has naturally seen the transfer of technology and equipment to this younger division of the aircraft industry. This is particularly so in the avionic and instrumentation area, but unfortunately it is not always possible to utilize directly the same equipment, owing to the unique characteristics of the helicopter. The simple and eminently suitable pitot-static system of airspeed measurement is not entirely adequate for the helicopter. The device is ineffective at airspeeds below 40 kts and does not function at all during rearward flight. A Doppler navigation system is no solution to the problem, since the apparently small error between ground speed and airspeed (airspeed = ground speed + wind speed) is sufficient to alter the flying characteristics to an extent which, if unknown by the pilot, could result in a fatal inappropriate use of the controls especially in emergency conditions when the pilot is under stress. Furthermore, with the increasing emphasis being placed on IFR flight and military missions, where ideal flight conditions cannot be guaranteed, accurate airspeed information is becoming more necessary. Rotor power requirements (essentially controlled by collective pitch at low speeds), cyclic stick sensitivity and pedal position are all substantially affected by small aerodynamic velocity changes. The area where airspeed is inaccurately or not known is depicted, taking into account helicopter side, rear and vertical velocity operating limits, in Figure 1.

Recognising the importance of this lack of instrumentation, the avionic equipment manufatureres have proposed and developed a number of solutions, most of which are based on the pitot-static principle but combine the weak unmeasurable velocity with one much stronger of known properties. Companies such as Marconi Elliot Ltd., J-TEC Associates Inc., Pacer Systems Inc. offer specially developed equipment for low airspeed measurement. However, since the flight characteristics of the helicopter are strongly affected by the airspeed, the possibility exists of estimating the velocity from a knowledge of the trim state of the helicopter. This paper presents an investigation of the theory, together with simulation results substantiating the method.

2. The Low Speed Flight Regime

Hovering and low speed flight is, by its very nature, probably one of the most frequented flight states of the helicopter. It is unfortunate that, in this region, the control characteristics, in the form of cyclic trim and power settings, are considerably altered by the aerodynamic flow through the rotor, thus making piloting in this most important flight state a taxing operation. In discussing this problem, it is useful to separate the fuselage and main rotor effects, in this case considering the tail rotor, fin and additional aerodynamic surfaces as belonging to the fuselage. For this idealisation, the rotor can be replaced by a simple thrust and moment generator.

Each different speed condition brings with it a new balance of forces, which result in a net zero acceleration of the helicopter. The aircraft is then said to be trimmed. The pilot finds this trim state by adjusting thrust magnitude and direction, but the most apparent indi-

cation of any changes is observed from the attitude of the fuselage. Even at low forward speeds, pitch attitude changes are discernible owing to the fuselage aerodynamic drag. In fact, if no drag existed, pitch attitude changes would not be necessary. In roll, however, the mechanics are somewhat complicated by the tail rotor thrust, which attempts to balance the main rotor torque, and is therefore dependent on the power requirements of the main rotor. The trim of the helicopter therefore, in particular the pitch attitude, is basically governed by the fuselage aerodynamics or more precisely by the ratio of the aerodynamic drag to the weight of the aircraft.

The main rotor on the other hand, which produces the thrust and moment, is governed by completely different principles. The rotor is always operating, from an aerodynamic viewpoint, at high speed, even in the hover. The addition of the helicopter's forward speed, for example, must be considered as an extension of the existing flow round the blades. In hover, the helicopter pilot regulates the controls, collective and cyclic blade pitch, in order to produce the thrust and moment required for trim. At this stage, the collective control can be considered as varying the thrust magnitude and cyclic as varying the thrust direction relative to the rotor shaft. Owing to mass centre position and the lateral tail rotor thrust, however, the cyclic control is rarely in the central position in order to trim the hover.

To execute a forward manoeuvre, the pilot briefly moves the cyclic stick forward, deflecting the thrust direction and so resulting in a nose down pitching moment. The helicopter accelerates, thereby changing the aerodynamic flow conditions round the rotor and, in particular, increasing the resultant velocity on the advancing blade. The advancing blade experiences a greater lift force and flaps upward approximately 90° later; depending on the rotor "stiffness". The process can be viewed as a tilt of the rotor disc (tip-path plane), or in classical helicopter terminology as the "rotor flap-back". The result is that, as the helicopter accelerates, there is a tendency for the rotor to automatically supply a moment which acts to oppose the motion. This static speed stability characteristic is only overcome by the pilot adjusting cyclic pitch on the advancing blade (and an equal and opposite amount on the retreating blade) which he does by moving the cyclic stick forward as the airspeed increases.

The situation is further complicated, especially in the low speed region, by the rotor flow dissymmetry between the leading and trailing edges of the rotor disc. In hover, the induced flow can be reasonably assumed to be uniform across the whole rotor disc. With an increase in forward speed, this assumption becomes wildly inaccurate. In practice, the leading edge of the disc receives a reduced downwash (in some cases a slight up-wash) and the trailing edge an increased downwash. The distortion of the induced velocity field by the forward speed has long been recognised and a trapezoidal model of the phenomenon, originally suggested by Glauert, is often used in theoretical analyses, where the computing time involved in more advanced vortex models is prohibitive. Figure 2 compares a typical induced velocity distribution with the simple Glauert model. The result of distortion of the flow field is that the angle of attack of a blade in the forward edge of the rotor disc is increased, thus producing an increase in lift. Taking into account the phase lag between the application of the aerodynamic force and blade flapping motion, maximum disc tilt is observed in the retreating blade

position. For a rotor with the conventional direction of rotation, this results in a positive roll to the right. The pilot counteracts this motion with a lateral cyclic control input.

Taking into account the effects of horizontal motion and asymmetric aerodynamic flow, the cyclic trim curve will be similar to Figure 3. In fact, owing to the aerodynamic flow effects, all single rotor helicopters will have a cyclic trim curve similar in shape to Figure 3, irrespective of helicopter mass, fuselage aerodynamics, rotor stiffness etc. To emphasize this point, the figure also shows the trim points for a hypothetical helicopter with no fuselage aerodynamics. The differences between the data points are negligible.

It can be concluded from this rather simplified explanation of the low speed flight regime, that the helicopter rotor itself provides a mechanism for estimating the airspeed, in particular from the measurement of control angles. The problem remains to develop a simple yet sufficiently detailed mathematical model, which can represent the flight mechanic behaviour of the rotor in this low speed region of interest.

3. Simplified Rotor Model

Current mathematical models of the helicopter rotor, as used in rotor performance, stability and blade dynamic calculations, have been developed over a number of years and, in an attempt to accurately predict the limits of the rotor, they have inevitably expanded dramatically in complexity (to include non-linear aerodynamics, blade couplings and elastic effects) in proportion to the computing capacity available. Consequently, their level of complexity, as required for modern rotorcraft design, renders them quite useless for the purposes of this paper which is to develop an inverse technique for calculating airspeed. Therefore, a much simplified model is required, remembering that non-linear effects need not be considered since, in the speed range of interest, the rotor will not be operating at any limiting condition.

Figure 4 shows a typical mathematical model of a rotor blade frequently used in computer programs for flight mechanics analysis. The elastic deformations of the rotor blade (semi-hingeless rotor) are represented by a number of theoretical hinges which, in general, contain associated stiffness and damping coefficients. In this way the model is able to represent the motions of the blade in the flapping, lagging and torsional degrees of freedom. From a flight mechanics point of view, the most important blade motion is flapping, which is retained in the second, much simplified, model in Figure 4. A further modification in this second model is that the theoretical flapping hinge is repositioned at the centre of the rotor shaft. In fact, for flight mechanics analysis, the most critical factor is not the positioning of the flapping hinge and the determination of the exact equivalent hinge stiffness, but the evaluation of the blade natural flapping frequency, which is both a function of the hinge position and spring stiffness. As Figure 5 shows, it is possible to interchange the flapping hinge position and spring stiffness of this theoretical model in order to match the measured frequency of the actual blade. With this much simplified model, it is now possible to obtain analytic expressions for the rotor thrust and disc tilt.

3.1 Rotor Disc Tilt

By equating moments about the theoretical flapping hinge and integrating along the total blade, the following second order differential equation is obtained for the flapping degree of freedom (see Figure 6).

$$\ddot{\beta}(\psi) + (\Omega^2 + \frac{c_\beta}{I_\beta}) \cdot \beta(\psi) + \Omega^2 \cdot \beta_I = \frac{1}{I_\beta} \cdot \int_0^R r \cdot dL + 2\Omega \cdot p \cdot \cos\psi - 2\Omega \cdot q \cdot \sin\psi \qquad (1)$$

From classical aerodynamic theory, the lift on a small blade element of radial length dr is,

$$dL = \frac{1}{2} \rho \cdot c \cdot V^2 \cdot c_L \cdot dr \qquad (2)$$

which in terms of normal and tangential velocity components acting on the blade, assuming linear aerodynamic theory and neglecting Mach number effects, can be written as,

$$dL = \frac{1}{2} \rho \cdot c \cdot a \, [U^2_T \cdot \theta(\psi, r) + U_T \cdot U_P] \cdot dr \qquad (3)$$

Non-dimensionalizing equation (1) (time w.r.t. rotor speed, velocity w.r.t. tip-speed) and introducing the concept of flapping natural frequency, the blade flapping equation becomes,

$$\ddot{\beta}(\psi) + \bar{\omega}_\beta \cdot \beta(\psi) + \beta_I = \frac{\gamma}{2} \int_0^1 [\bar{U}_T^2 \cdot \theta(\psi, x) + \bar{U}_T \cdot \bar{U}_P] \cdot x \cdot dx + 2\bar{p} \cdot \cos\psi - 2\bar{q} \cdot \sin\psi \quad . \qquad (4)$$

It now only remains to enter the aerodynamic velocity components as represented diagramatically in Figure 7 and solve equation (4) to obtain an expression governing the angle of the rotor tip-path plane relative to the rotor shaft (disc tilt). It is at this stage, of course, that the helicopter forward and lateral velocities enter the problem, by introducing sinusoidal and cosinusoidal harmonic components respectively in the blade tangential direction (U_T). Solving equation (4) and equating harmonic components, the first harmonic longitudinal disc tilt (β_{1c}) and first harmonic lateral disc tilt (β_{1s}) can be found. For a more detailed treatment of this brief derivation the reader is referred to references such as (1), (2), (3) or (4).

3.2 Rotor Thrust

Having derived the expression for rotor flapping, the thrust follows simply from integrating equation (3) with respect to rotor radius, averaging for a complete rotor revolution and summing for n blades.

$$T = \frac{n}{2\pi} \cdot \int_0^{2\pi} \int_0^{R} dL \cdot d\psi \qquad (5)$$

or

$$C_T = \frac{a \cdot \sigma}{2\pi} \cdot \int_0^{2\pi} \int_0^{1} [\bar{U}_T^2 \cdot \theta(\psi, x) + \bar{U}_T \cdot \bar{U}_P] \cdot dx \cdot d\psi \qquad (6)$$

Hence, from equation (6) a simple analytic expression for the thrust is obtained.

3.3 Tuning the Simplified Rotor Model

The analytic expressions derived from equations (4) and (6) can be used instead of the more complete model shown in Figure 4 (with some limitations), but the model parameters have to be selected in order to obtain comparable results. This "tuning" operation is not as difficult as might be imagined, since all the rotor characteristics have been reduced to a few non-dimensional parameters and a detailed description of the blade geometry is not required. For example, as already discussed, it is only necessary in this model to define the blade flapping frequency $\bar{\omega}_\beta$ and not hinge off-set and spring stiffness. The parameters to be adjusted are,

- $\bar{\omega}_\beta$ blade flapping frequency
- γ Lock's number (also used as $\gamma/8$, blade mass number (n_β))

and

- a average lift-curve slope of blade profile.

In practice, flapping frequency is already defined by measurement, or from a blade dynamics program, and need not be included in this parameter investigation. The remaining two parameters can be defined assuming linear mass distribution and from simple 2-dimensional aerofoil theory and can be refined by a curve fitting exercise. Figure 8 shows the general trends of these parameters and compares the cyclic trim angles for both a comprehensive rotor analysis and the simplified model. It should be pointed out that the exclusive use of the simple analytic model for flight mechanic investigations is not possible, since factors such as aerodynamic stall, Mach number, elastic deformations etc. are not included. The simplified model cannot be used as a substitute for the full rotor model in design calculations.

3.4 Inversion of the Rotor Equations

Having established in the previous section that a simple analytic representation of the rotor system can produce comparable trim curves (certainly within the present speed range of interest) to a fully non-linear description of the rotor, it is possible to re-arrange the equations to obtain explicit expressions for the in-plane velocity components $\bar{V}_x$ and $\bar{V}_y$;

$$\bar{V}_x = \bar{f}_x - \bar{f}_z \cdot \bar{f}_y \qquad (7)$$

$$\bar{V}_y = \bar{f}_z \cdot \bar{f}_x + \bar{f}_y$$

where $$\bar{f}_x = \frac{S_\beta \cdot \beta_{1s} - \beta_{1c} - \theta_{1s} - \bar{p} + \frac{2}{n_\beta} \cdot \bar{q} + E_y \cdot \bar{V}_{Io}}{\theta_t + \frac{4}{3}\theta_o + \frac{4C_T}{a \cdot \sigma}} \quad (8)$$

$$\bar{f}_y = \frac{\beta_{1s} + S_\beta \cdot \beta_{1c} - \theta_{1c} - \frac{2}{n_\beta} \cdot \bar{p} - \bar{q} + E_x \cdot \bar{V}_{Io}}{\theta_t + \frac{4}{3}\theta_o + \frac{4C_T}{a \cdot \sigma}} \quad (9)$$

$$\bar{f}_z = \frac{\frac{4}{3}(\beta_I + \beta_o)}{\theta_t + \frac{4}{3}\theta_o + \frac{4C_T}{a \cdot \sigma}} \quad (10)$$

In deriving the above equations, terms in $\bar{V}^2$ and higher order as well as other small quantities have been neglected. As will be discussed in a following section, in some instances these equations can be further simplified, depending on the application, without significant loss of accuracy. The basic parameters which need to be measured are the rotor control angles (θ) and the rotor disc tilt (β).

4. The Velocity Observer

4.1 Sensitivity Analysis

An initial sensitivity analysis of the velocity observer equations (7) to (10) derived in section 3 indicates the relative importance that must be placed on the various terms (see Figure 9). It should be noted that the word observer is used here in a more general sense and does not imply the more specialized meaning used in linear control theory. The analysis shows that by incrementing the angular variables in turn by 1^o (typically 30% of the total trim cyclic range between ± 20 m/s, see Figure 3), cyclic control angles (θ_{1s}, θ_{1c}) and disc tilt have the most significant influence on the calculated speed. Blade coning (β_o) and inbuilt coning angle (β_I), together with collective, are of less importance. Pitch and roll angular rates of 10% (typically half the peak value obtained during a rapid acceleration manoeuvre) are shown to be significant. Nominal values for the downwash distribution parameters ($E_x \cdot V_{Io}$, $E_y \cdot V_{Io}$) show that the resulting error necessitates their inclusion but changes in rotor thrust, which are not considerable during normal level flight, can be neglected.

4.2 Dynamic Performance

The foreseen application for the velocity observer is as an aid during hovering and low speed manoeuvreing, as well as during acceleration manoeuvres, where speed dependent flight characteristics can cause piloting difficulties under certain conditions as discussed in section (1). Comparison of the two rotor models has demonstrated the static accuracy of the method. A further analysis is, however, required to investigate the inaccuracies involved in the dynamic situation.

A typical horizontal acceleration manoeuvre is shown in Figure 10. A pilot model was developed for the simulation, such that, from trimmed hover, an acceleration was produced with constant altitude and using up to 95% of available engine power (continuous ratings). After reaching approximately 20 m/s, the acceleration is terminated and speed and altitude maintained.

Figure 11 compares the forward horizontal speed predicted by the velocity observer with the simulated manoeuvre. A reduced set of decoupled equations was used in this case (ie. $\bar{f}_z = 0$ in equations (7)). In fact, the $\bar{f}_z$ term has a value of about 0.2 under normal circumstances and can be neglected in this discussion of the system principle. Comparisons between the velocity calculation and the simulated manoeuvre show very encouraging results. The trends of the two curves are the same and the displayed errors would be perfectly acceptable in an operational system. The pitch rate term is shown to have a considerable effect, as was anticipated in the sensitivity analysis (Figure 9). For certain applications, where the mission does not require violent manoeuvres (e.g. a large transport helicopter), it might be possible to omit the angular velocities without causing appreciable error. Exact measurement of blade collective angle is shown not to be critical.

In the lateral axis (Figure 12), the velocity is estimated with reasonable accuracy. The principal error shown here is caused by not taking into account the non-linear induced velocity distribution. Owing to cross-coupling effects, the exclusion of pitch rate in the method results in a transient error similar to that shown in Figure 11.

By further adjustment of the model and the inclusion of the cross-coupling function $\bar{f}_z$, the observer can be tuned to produce improved results (Figure 13).

Vertical velocities (e.g. an acceleration plus climb) do, however, result in errors (Figure 14), but as these occur at substantial vertical velocities it should be possible, if required by the mission, to include compensation as a function of vertical speed (e.g. from a Doppler system).

5. System Realization

The discussion of the velocity observer in section (4) has demonstrated the requirement for the measurement of,

- control angles, cyclic (θ_{1s}, θ_{1c}) and collective (θ_o)
- pitch and roll rates (p, q)
- angle of tip-path plane relative to rotor shaft (β_{1s}, β_{1c})

and

- approximate rotor thrust (helicopter weight).

Control angles and angular rates present no great problems and are normally parameters already available as part of the flight control system. In the case of a helicopter with a conventional articulated rotor, it is conceivable to measure blade flap angle directly at the flapping hinge. Where no physical hinge exists, it is possible to measure directly flapp-

ing moment, which can be related to the flapping angle through a simple "stiffness" constant. For other reasons, a rotor hub moment sensor is already a standard fit on the MBB BO 105 helicopter, peak moment values being displayed to the pilot on the central instrument panel. Typical raw data from the sensor is shown in Figure 15. The measured signal is not of course the theoretical one-per-rev sinusoidal oscillation (the sensor is fixed to the rotating shaft), but includes distortions owing to the higher harmonic blade flapping modes. However, knowing the frequency and phase angle, it is not difficult to process the data for the 1Ω content and hence obtain the required harmonic coefficients β_{1s} and β_{1c}. Figure 16 shows a block diagram of a practical system.

It is worth pointing out that, since both rotor inputs (blade pitch) and rotor response (disc tilt) are directly measured, the helicopter's mass-centre position does not affect the results.

6. Further Study

The usefulness of the proposed system will only be proven by flight test. Experimental investigations are currently under way which are hoped to be reported in a further paper.

7. Conclusions

A method has been postulated by which the aerodynamic speed of the helicopter can be estimated from a knowledge of the rotor control angles and rotor tip-path plane (disc tilt). Investigation of the method through simulation and analysis has shown that it should be possible to obtain both longitudinal and lateral velocity components with reasonable accuracy (certainly better than conventional pitot-static-systems).

8. References

1) A. Gessow, G.C. Myers, Aerodynamics of the Helicopter, Frederick Ungar Publishing Co., 1967

2) -, Helicopter Aerodynamics and Dynamics, AGARD Lecture Series No.63, 1973

3) A.R.S. Bramwell, Helicopter Dynamics, Edward Arnold, 1976

4) P.R. Payne, Helicopter Dynamics and Aerodynamics, Sir Isaac Pitman & Sons Ltd., 1959

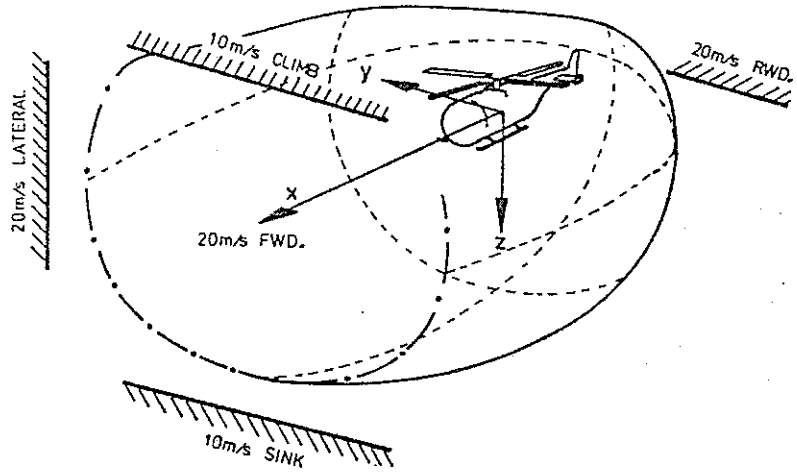

Figure 1 Low Speed Flight - Typical Velocity Limits -

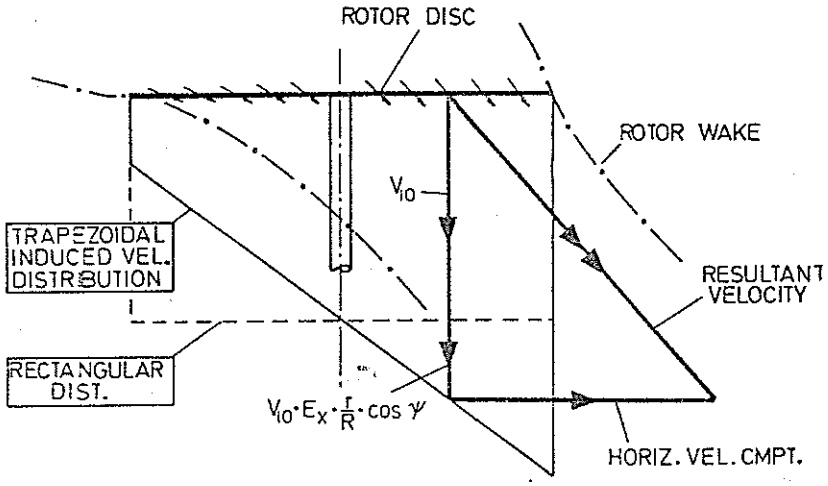

Figure 2 Aerodynamic Flow through the Rotor

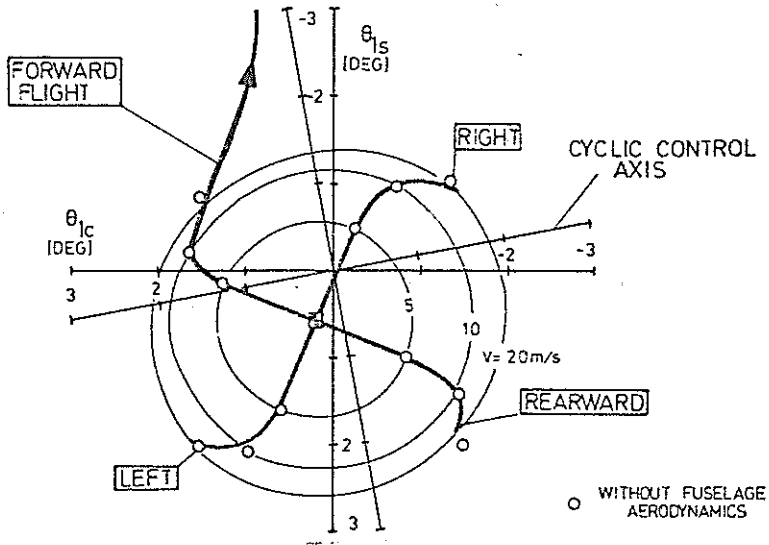

Figure 3 Cyclic Control Requirements for Trim

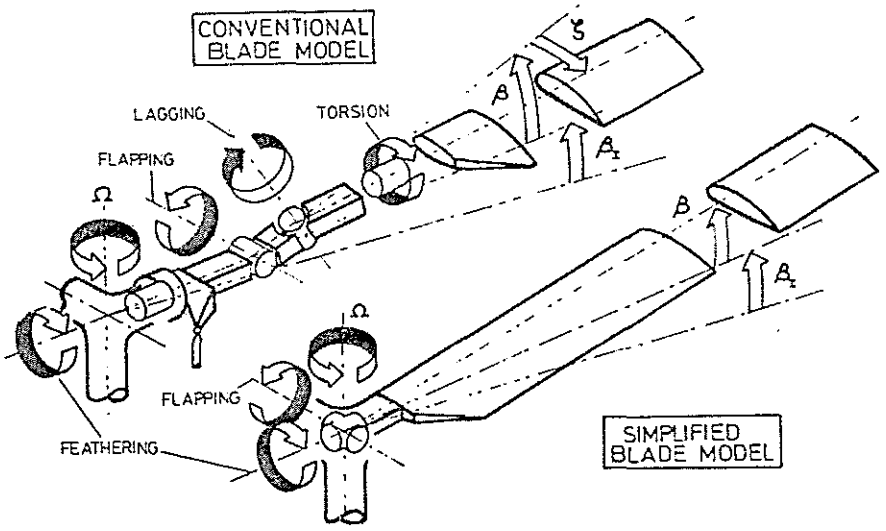

Figure 4 Comparison of Rotor Blade Models

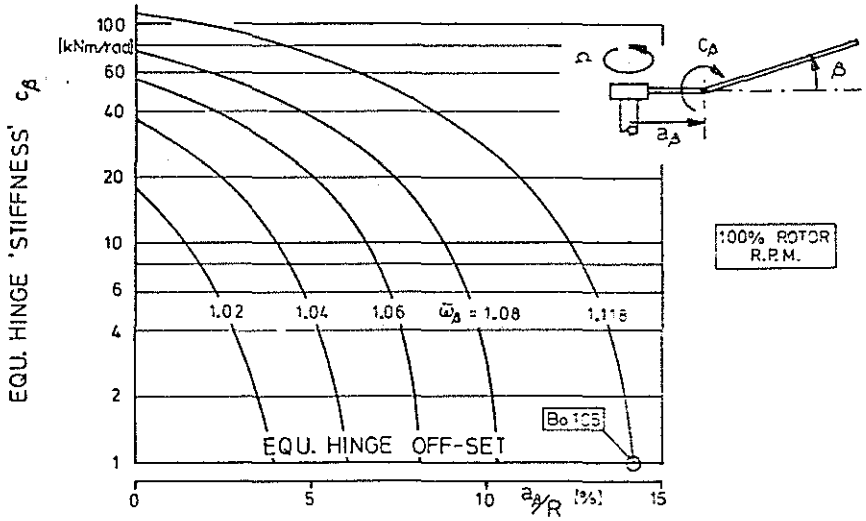

Figure 5 Equivalence of Hinge "Stiffness" & Hinge Off-set

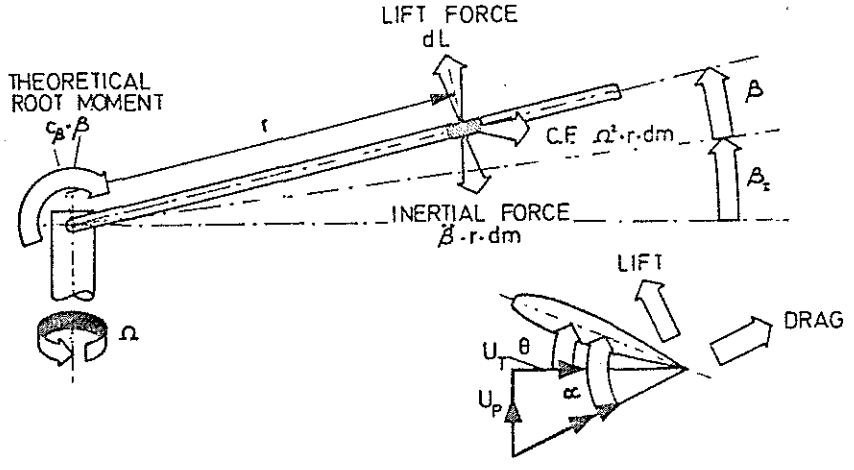

Figure 6 Forces Acting on a Blade Element

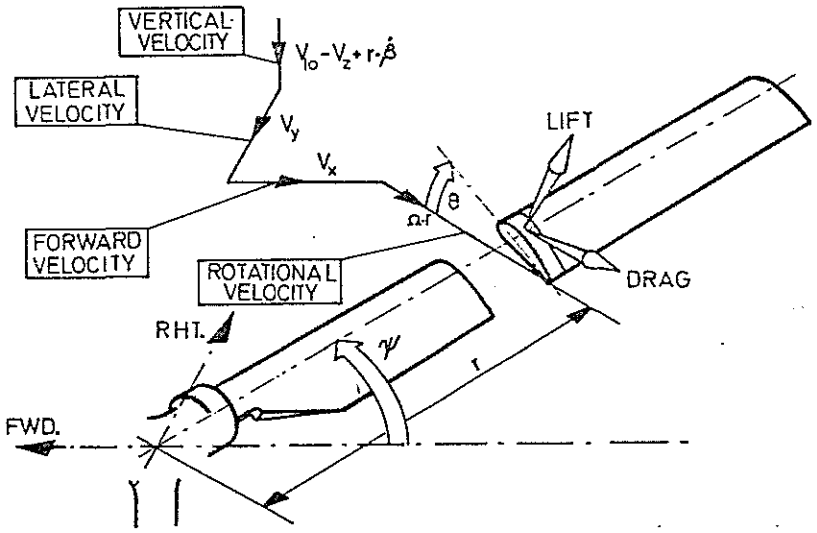

Figure 7 Velocity Vector on a Blade Element

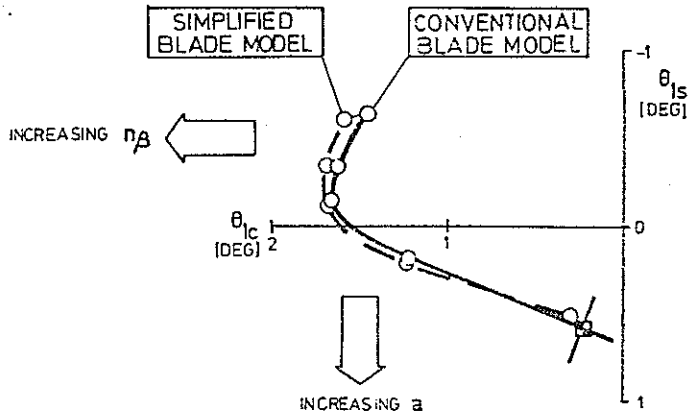

Figure 8 Fitting of Simplified Blade Model

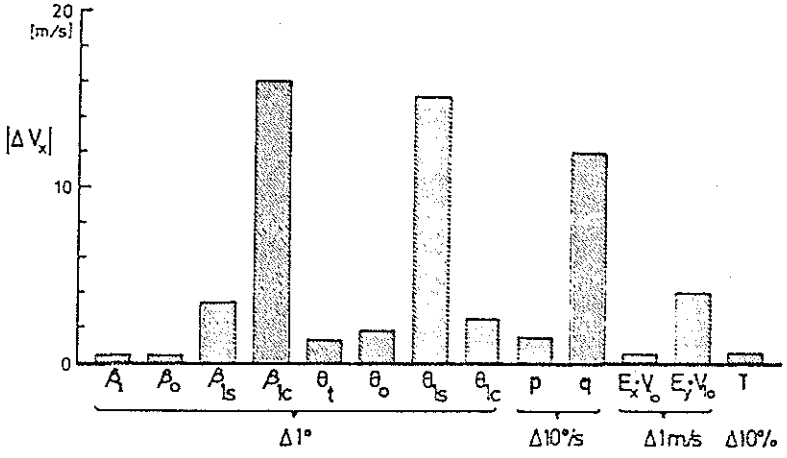

Figure 9 Sensitivity of Measurement Error on Calculated Airspeed

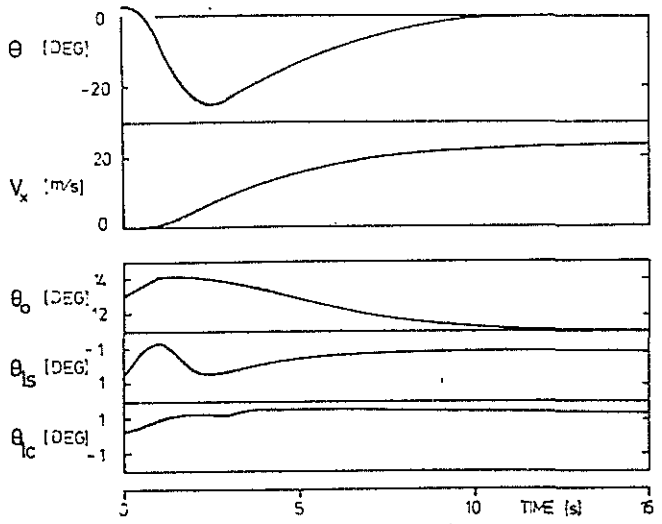

Figure 10 Typical Acceleration Manoeuvre at Constant Altitude

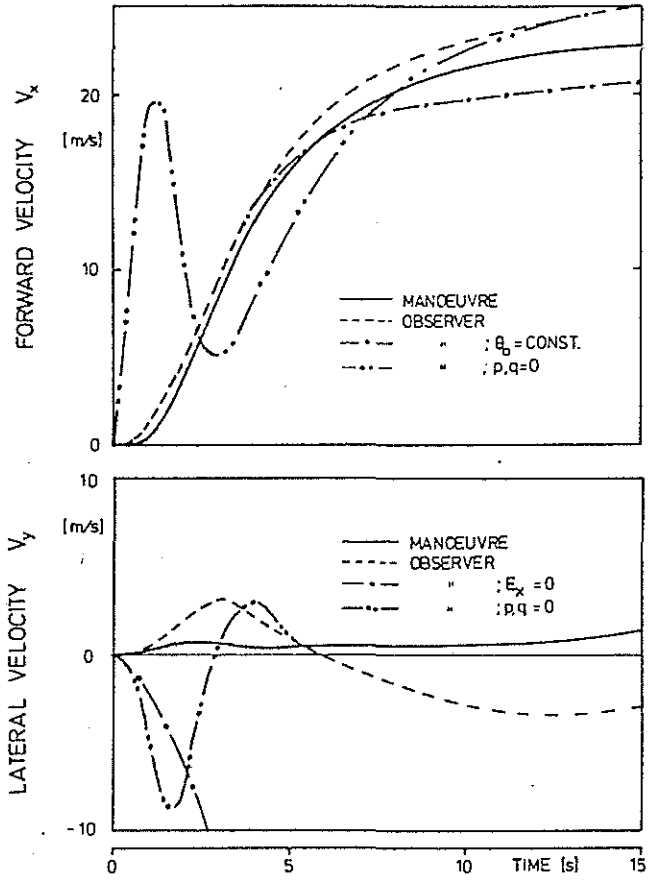

Figure 11 & 12 Comparison of Simulated Manoeuvre and Velocity Observer Method

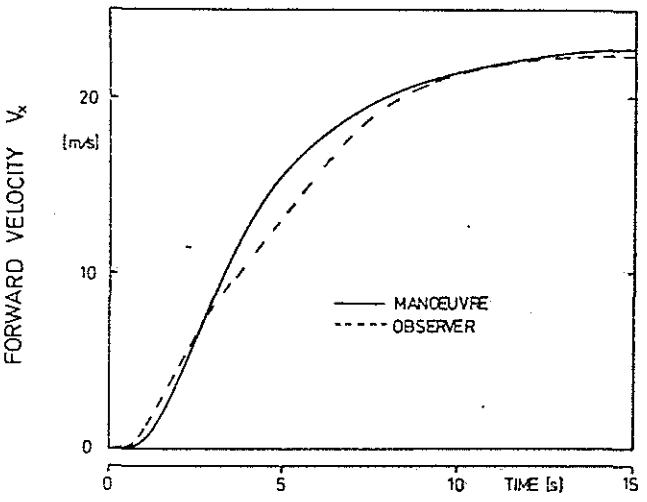

Figure 13 Velocity Observer Method Showing Improved Results

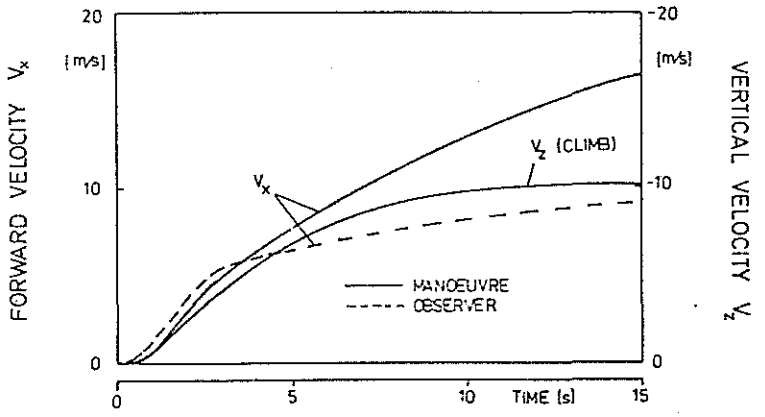

Figure 14 Predicted Velocity During a Climb Manoeuvre

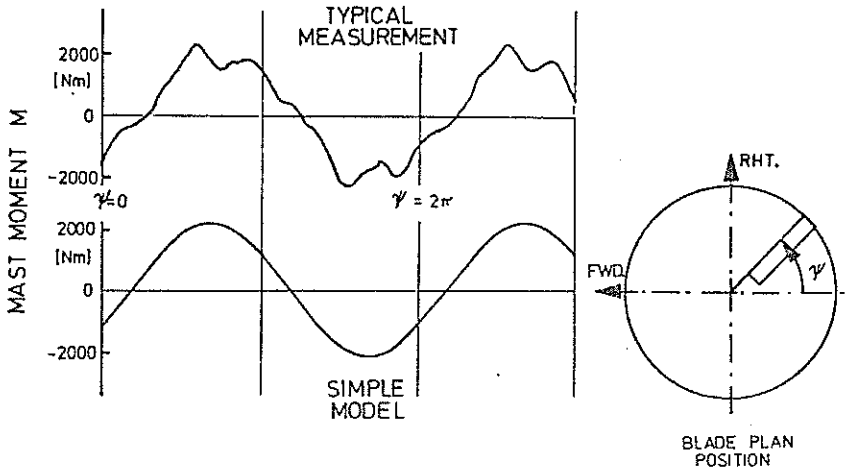

Figure 15 Rotor Mast Moment vs. Rotor Azimuth Angle

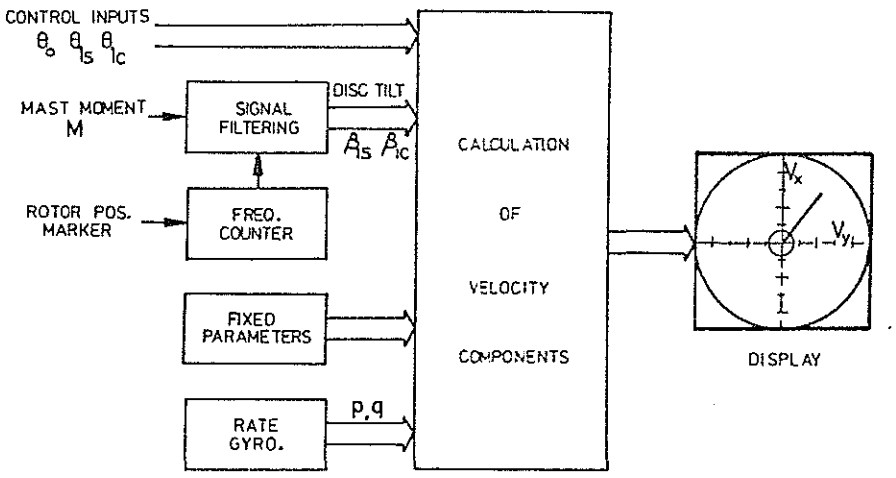

Figure 16 Block Diagram of Velocity Observer